

## Supported metal electronic structure: Implications for molecular adsorption

Valentino R. Cooper, Alexie M. Kolpak, Yashar Yourdshahyan, and Andrew M. Rappe\*  
*The Makineni Theoretical Laboratories, Department of Chemistry, University of Pennsylvania,  
 231 South 34th Street, Philadelphia, Pennsylvania 19104-6323, USA*

(Received 22 November 2004; revised manuscript received 17 May 2005; published 29 August 2005)

Using *ab initio* methods, we examine the electronic structure of substrate-supported metal films. We predict a coexistence between charge-transfer valence-bond states and bandlike metallic states. The role of the support composition in determining the balance of bond and band states is elucidated for Pt on Al- and O-terminated  $\alpha$ -Al<sub>2</sub>O<sub>3</sub>, and we reveal how this coexistence evolves with metal film thickness. Using CO chemisorption as a probe of metal film electronic structure, we demonstrate that this combination of bond and band effects leads to significant changes in surface chemistry.

DOI: [10.1103/PhysRevB.72.081409](https://doi.org/10.1103/PhysRevB.72.081409)

PACS number(s): 68.43.Bc, 68.43.Fg, 68.47.-b, 82.65.+r

The electronic structure of thin metal films is sensitive to boundary conditions, such as interactions with an oxide support. For sufficiently thin films, the electronic structure response to the support material can qualitatively change the physical and chemical properties at the surface of the film. An understanding of how the support material alters the properties of the metal can suggest alternate methods for tuning the activity at the metal surface. Such knowledge will allow for the creation of more efficient catalysts for manufacturing processes, fuel combustion, and the treatment of automotive exhausts and for the production of more sensitive chemical sensors.

Numerous theoretical and experimental studies have suggested that the support material plays an important role in tuning the reactivity at the surface of the metal nanoparticles.<sup>1-6</sup> For example, early studies of Pt on ZnO showed that the support termination (Zn or O) has a significant influence on the desorption of CO from the Pt surface.<sup>7</sup> Later studies suggested that this change in desorption temperature is due to differences in charge transfer at the different metal-oxide support interfaces.<sup>8</sup> In addition, many studies indicate that the size and shape of the nanoparticle as well as direct adsorbate-support interactions are important contributing factors to the metal surface reactivity.<sup>5,9-14</sup> However, separating the effects of the support-metal interactions from nanoparticle size and shape effects and direct adsorbate-support interactions is not trivial. The first experimental study to eliminate the latter two effects was recently performed by Chen and Goodman,<sup>15</sup> in which they used a thin film geometry to investigate the influence of a TiO<sub>2</sub> support on the reactivity of Au. Their study showed that charge transfer between the support and the metal catalyst significantly affects the reactivity at the metal surface.

Adsorbate-metal interactions can be characterized by a simultaneous transfer of electrons from the adsorbing molecule into unoccupied metal states (direct bonding) and a back donation of electrons from occupied metal states into the adsorbate orbitals. For transition metal surfaces, this exchange is achieved through interactions with the *d* orbitals of the metal. Previous work of Hammer and Nørskov showed that molecular chemisorption can be predicted solely by observing shifts in the center of the total *d*-band density of states (DOS) of the metal.<sup>16,17</sup> While this method has been

successfully applied to a number of unsupported metal surfaces, it cannot describe complicated rearrangements in the population and energy levels of the DOS of the surface *d* orbitals which may result from covalent or metallic bonding present at the metal-support interface. Such modifications of the metal surface *d* orbitals can have a considerable influence on molecular adsorption by altering the direct- and back-bonding interactions at the surface.

In this paper, we present a systematic study of the electronic structure of Pt thin films, and its modification due to interactions with two  $\alpha$ -alumina substrates with different electronic properties. We use density functional theory<sup>18,19</sup> (DFT) calculations and orbital-projected DOS to demonstrate how changes in the support affect each of the metal *d* orbitals. We then apply these results to demonstrate how the electronic structure trends of supported films give rise to anomalous chemisorption trends with respect to film thickness and substrate. The thin film geometry used in this study excludes particle shape and direct support interactions, allowing us to concentrate on the effect of the metal-support interactions on the metal surface reactivity. We observe dramatic differences in the electronic properties at the metal surface in Pt films of 1–5 atomic layers deposited on oxide supports with different electronegativities, emphasizing the importance of the underlying support. In particular, we show that support-metal interactions can create localized covalent bonds, whose character varies with the support surface. These bond-valence states evolve with Pt film thickness differently from the underlying metallic band states, leading to a rich dependence of electronic structure on film thickness.

To elucidate this rich surface chemistry we constructed a model based on second-order perturbation theory:

$$E_{\text{Chem}} = 2 \int_{-\infty}^{\varepsilon_F} \frac{n_{d_\pi}(\varepsilon) |V_\pi|^2}{\varepsilon_{2\pi^*} - \varepsilon} d\varepsilon + 2 \int_{\varepsilon_F}^{+\infty} \frac{n_{d_\sigma}(\varepsilon) |V_\sigma|^2}{\varepsilon - \varepsilon_{5\sigma}} d\varepsilon - \alpha. \quad (1)$$

Here  $n_{d_\pi}(\varepsilon)$  and  $n_{d_\sigma}(\varepsilon)$  are the number of *d* states of eigenenergy  $\varepsilon$  and correct symmetry to interact with the CO  $2\pi^*$  and  $5\sigma$  orbitals, respectively. The first term in this equation corresponds to the energy gained from the back donation of electrons from the metal *d* <sub>$\pi$</sub>  orbitals to the CO  $2\pi^*$  orbitals,

while the second term measures the gain in energy from the exchange of electrons from the CO  $5\sigma$  to the metal  $d\sigma$  orbitals.  $V_\pi$  and  $V_\sigma$  represent the coupling matrix elements for back donation and direct donation of electrons between the metal surface and the CO  $2\pi^*$  and  $5\sigma$  orbitals, respectively. Similar to the arguments presented by Hammer and Nørskov,<sup>16,17</sup> this model allows us to correlate trends in the metal's DOS to changes in the chemisorption energy of a molecule to the metal surface. The important differences are as follows: the integrals are only over filled or empty states (as appropriate for the particular interaction), only the specific metal  $d$  orbital involved in bonding at a particular site with a specific CO orbital is considered, and the integral reflects the bonding strength of each part of the DOS. CO  $\sigma$  bonding is due to interactions with empty  $d_{z^2}$  states at the top site and empty  $d_{xy}$  and  $d_{x^2-y^2}$  states at the hollow site. CO  $\pi$  bonding at both sites is with the filled metal  $d_{xz}$  and  $d_{yz}$  states.

We examine metal-oxide interfaces of different electronegativities by considering two variants of the  $\alpha$ -alumina surface: the Al-terminated surface ( $\text{Al}_T$ ), which is the most stable clean surface,<sup>20</sup> and the strongly polar O-terminated surface ( $\text{O}_T$ ), which is stable when hydrogen or a supported metal is adsorbed.<sup>21</sup> We use a slab geometry with an in-plane  $(\sqrt{3} \times \sqrt{3})R30^\circ$  unit cell and periodic boundary conditions to model the alumina surface.<sup>22</sup> The layer stacking can be represented by the formula  $(\text{Al-O}_3\text{-Al})_4\text{-Al-O}_3\text{-Al}_m\text{-(Pt}_3)_n$ , where  $m=0$  or 1 for the  $\text{O}_T$  and  $\text{Al}_T$  surfaces, respectively, and  $n$  is the number of Pt layers. For both terminations, the interfacial Pt atoms are in the energetically preferred registry, directly above the surface O atoms, forming a Pt(111) film. All calculations were performed using DFT with the generalized gradient approximation<sup>23</sup> for the exchange correlation functional, as implemented in the dacapo code,<sup>24</sup> with a plane-wave cutoff of 30 Ry, ultrasoft pseudopotentials,<sup>25</sup> and a  $2 \times 2 \times 1$  Monkhorst-Pack  $k$ -point mesh.<sup>26</sup> All slab calculations were performed with at least 12 Å of vacuum between periodic images in the [0001] direction. Total energies were tested to ensure that there were no surface interactions through the slab or the vacuum. The theoretical  $\alpha\text{-Al}_2\text{O}_3$  in-plane lattice constant of 4.798 Å was used [experimental = 4.759 Å (Ref. 27)]. In order to eliminate strain effects, all adsorption energies were compared to unsupported Pt(111) calculations at the same in-plane geometry as the supported metal. [This corresponds to the experimental Pt(111) in-plane lattice constant of 2.77 Å.] For our simulations, we fixed the ions in the bottom two alumina layers to their theoretical positions, relaxed the third layer perpendicular to the surface, and fully relaxed the remaining alumina layers, Pt layers, and adsorbates until the remaining force on each atom was less than 0.01 eV/Å. We correct for known DFT CO chemisorption errors<sup>28,29</sup> using the extrapolation method of Mason and coworkers<sup>30</sup> and have estimated chemisorption error bars of 0.02 eV.

Figure 1 shows the projected DOS of the surface Pt atoms for one and two layers of Pt deposited onto an  $\text{Al}_T$ -alumina surface. The  $\text{Al}_T$  surface is slightly electropositive, so when metal is deposited onto the oxide support, the metallic bands formed at the interface are affected by charge transfer from

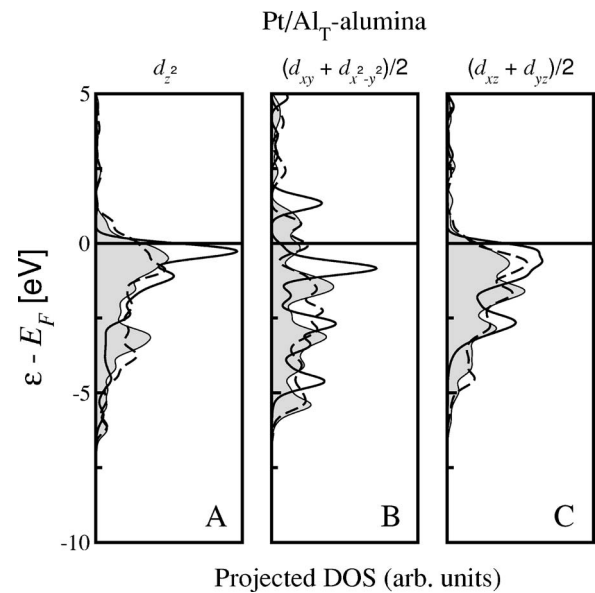


FIG. 1. The orbital-projected DOS plots for the surface Pt atoms for the Pt/ $\text{Al}_T$ -alumina system. The shaded regions represent the Pt(111) surface, the solid (—) lines are for the monolayer and the dashed (---) lines are for the bilayer.

the surface Al atoms into the metal atoms. For a single layer of Pt atoms on the  $\text{Al}_T$  surface, this charge transfer reduces the number of free states in all five  $d$  orbitals, relative to unsupported Pt(111), increasing the electron-electron repulsions within these orbitals and shifting the filled DOS upward in energy. Table I shows the changes in binding energy due to  $\pi$  and  $\sigma$  bonding at top and hollow sites as predicted by a fit of our model to DFT calculations. Here, our model shows that the upward shifts in the filled DOS of the  $d_{xz}$  and  $d_{yz}$  orbitals results in strong  $\pi$  bonding at both top and hollow sites. This greatly enhances the bonding of CO to the Pt surface, relative to Pt(111). On the other hand, changes in the number of unoccupied states of the remaining orbitals weakens  $\sigma$  bonding at the hollow site ( $d_{xy}$  and  $d_{x^2-y^2}$  states) [relative to Pt(111)] more than at the top site ( $d_{z^2}$ ).

To form the bilayer Pt/ $\text{Al}_T$  system, the second layer Pt atoms occupy hollow sites of the interfacial Pt layer. This arrangement allows for interactions between the  $d$  orbitals of the surface and interfacial Pt atoms. The resulting metallic bands still show some influence of the interface. The charge transfer from Al atoms decreases the number of free second-layer  $d_{xz}$ ,  $d_{yz}$ ,  $d_{xy}$ , and  $d_{x^2-y^2}$  states and causes an upward shift in the energy of the occupied states relative to Pt(111) [Figs. 1(b) and 1(c)], but these effects are smaller than for monolayer Pt/ $\text{Al}_T$ . Our model indicates that the shifts in unoccupied  $d_{xy}$  and  $d_{x^2-y^2}$  results in relatively little change in the  $\sigma$  bonding at the hollow site, while the upward shift in the energy of the  $d_{xz}$  and  $d_{yz}$  states strengthens bonding at both top and hollow sites. The  $d_{z^2}$  orbital points into the hollow site and therefore does not interact strongly with the underlying interfacial Pt atoms. In response to increased electron-electron repulsion due to greater population of the other  $d$  orbitals, the  $d_{z^2}$  orbital loses a fraction of an electron, resulting in more free  $d_{z^2}$  states. This population reduction results in the formation of stronger  $\sigma$  bonds with CO. In this

TABLE I. Changes in  $\sigma$  and  $\pi$  bonding relative to Pt(111), and total  $E_{\text{Chem}}$  for CO adsorption to top and hollow sites for the Pt/ $\alpha$ -Al<sub>2</sub>O<sub>3</sub> system. Al-terminated (Al<sub>T</sub>) and O-terminated (O<sub>T</sub>) supports are considered, and various Pt layer thicknesses are studied. The model of equation (1) [ $\sigma$ - and  $\pi$ -bonding contributions and total (Ref. 33)] is compared with first-principles calculations for all systems. All energies are in eV (Ref. 31).

System	Top site				Hollow site			
	$\sigma$	$\pi$	$E_{\text{chem}}$	$E_{\text{chem}}$	$\sigma$	$\pi$	$E_{\text{chem}}$	$E_{\text{chem}}$
1L Pt/Al <sub>T</sub>	-0.04	1.28	2.53	2.55	-0.16	1.19	2.26	2.28
2L Pt/Al <sub>T</sub>	0.05	0.31	1.66	1.61	0.02	0.24	1.48	1.33
3L Pt/Al <sub>T</sub>	0.00	0.06	1.37	1.47	-0.07	0.03	1.16	1.36
4L Pt/Al <sub>T</sub>	0.00	0.01	1.32	1.30	0.03	0.01	1.27	1.21
5L Pt/Al <sub>T</sub>	-0.01	0.02	1.32	1.30	0.00	0.01	1.24	1.25
1L Pt/O <sub>T</sub>	0.79	-0.13	1.95	1.97	-0.28	-0.13	0.82	0.74
2L Pt/O <sub>T</sub>	-0.13	-0.14	1.05	1.09	0.24	-0.26	1.21	1.21
3L Pt/O <sub>T</sub>	0.05	0.01	1.37	1.35	0.03	0.04	1.29	1.32
4L Pt/O <sub>T</sub>	-0.02	0.04	1.34	1.32	0.00	0.04	1.27	1.29
5L Pt/O <sub>T</sub>	0.00	0.02	1.34	1.35	0.04	0.03	1.30	1.31
Pt(111)			1.31	1.28			1.22	1.24

case, the increase in  $d_{z^2}$   $\sigma$  bonding explains the strong preference towards top site binding (Table I). For three or more layers of Pt, the DOS of the surface atoms returns to the Pt(111) values, and therefore adsorbate-metal interactions will be similar to those on the unsupported metal.

Figure 2 shows the projected DOS of the surface Pt atoms for one and two layers of Pt deposited onto an O<sub>T</sub>-alumina surface. The absence of Al atoms on this surface leaves the surface oxygen ions electron deficient. When a layer of Pt atoms is deposited onto this electronegative surface, partially ionic covalent bonds are formed between the oxygen  $p$  orbitals and the Pt  $d$  orbitals. Since the Pt atoms are deposited

directly on top of oxygen ions, valence-bond states (hybrid orbitals) are formed with metal  $d$  orbitals with components perpendicular to the oxide surface ( $d_{z^2}$ ,  $d_{xz}$ , and  $d_{yz}$ ). In the case of the  $d_{z^2}$  DOS [Fig. 2(a)] the creation of hybrid orbitals in the monolayer system causes a splitting of these states, producing a higher energy unoccupied antibonding orbital ( $\sim 1$  eV above the Fermi level) and a much lower energy occupied bonding orbital ( $\sim 6$  eV below the Fermi level). This splitting greatly increases the number of free  $d_{z^2}$  states, while shifting the energy of the occupied states downward. As a result, there is an increase in  $\sigma$  bonding with the  $d_{z^2}$  at the metal surface, which corresponds to the large increase in the CO top site chemisorption energy. The  $d_{xz}$  and  $d_{yz}$  orbitals also form covalent bonds with the oxygen  $p$  orbitals. These new valence-bond states are manifested in the decrease in states with energies between 0.0 and  $-2.5$  eV relative to the Fermi level and an increase in states with energies below  $-5.0$  eV, with little or no change in the number of free states in these orbitals. While the  $d_{xy}$  and  $d_{x^2-y^2}$  do not form hybrid orbitals with the oxygen orbitals, the loss of electrons in the other  $d$  orbitals reduces the electron-electron repulsions with these states. This shifts their filled DOS downward relative to Pt(111), while shifting the free states to higher energies. In this system, both  $\pi$  bonds with the Pt  $d_{xz}$  and  $d_{yz}$  and  $\sigma$  bonds with the metal  $d_{xy}$  and  $d_{x^2-y^2}$  are dramatically weaker. These effects are manifested in the huge site preference for the single layer Pt/O<sub>T</sub> system (Table I).

Similar to the bilayer of Pt/Al<sub>T</sub>, the second layer Pt atoms on the O<sub>T</sub> surface occupy hollow sites of the interfacial Pt atoms as in a (111) fcc surface. This again allows the  $d$  orbitals of the interfacial Pt atoms to directly interact with the  $d_{xz}$ ,  $d_{yz}$ ,  $d_{xy}$ , and  $d_{x^2-y^2}$  orbitals of the second layer atoms, forming metallic bands. Here, the  $d_{xz}$  and  $d_{yz}$  orbitals exhibit a slight downward shift in the metal DOS relative to Pt(111), thereby weakening  $\pi$  bonding at top and hollow sites. The shifts in the  $d_{xy}$  and  $d_{x^2-y^2}$  orbitals increase the number of

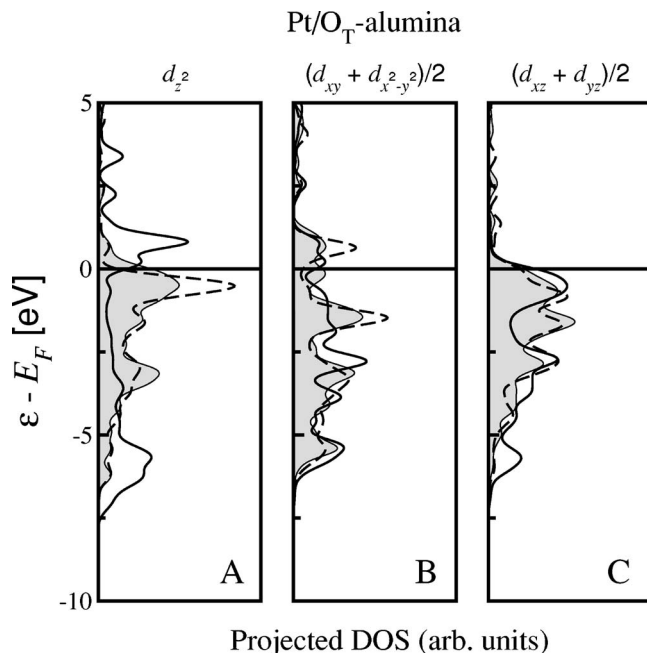


FIG. 2. Same as Fig. 1, for Pt/O<sub>T</sub>-alumina system.

free states while having no effect on the center of occupied states. This will result in stronger direct  $\sigma$  bonding with these orbitals. The combination of  $\sigma$  and  $\pi$  bonding at the hollow site results in little change in the CO chemisorption energy, relative to Pt(111). In response to decreased electron-electron repulsion due to smaller population of the other  $d$  orbitals, the  $d_{z^2}$  orbital gains a fraction of an electron, resulting in a dramatic reduction in free  $d_{z^2}$  states. This charge transfer into  $d_{z^2}$  also causes an upward shift in the filled  $d_{z^2}$  DOS due to strong electron-electron repulsions within the  $d_{z^2}$  orbitals. These changes weaken  $\sigma$  bonds with CO. The large weakening of top site binding and the small difference in hollow site binding result in a change to the hollow site being preferred for Pt/ $O_T$  bilayers. For three or more layers of Pt, the DOS of the surface atoms returns to Pt(111) values, and therefore we expect the adsorbate-metal interactions will resemble those of the unsupported metal.

We have shown how metallic and covalent bonding at the metal-support interface affect the orbital-specific electronic structure of the surface Pt layer. Furthermore, we show how a simple second-order perturbation theory model can be used to interpret how these changes will affect the metal's interaction with molecular adsorbates. Our results present a theoretical basis for understanding the interactions between an oxide support and a supported metal film. We show that the oxide terminations of different electronegativities result in different bonding mechanisms at the metal-support interface, and that a mixture of both covalent and metallic bonds produces interesting surface chemistry in subsequent layers. The very different CO adsorption behavior as a function of Pt film thickness for the two surface terminations confirms the idea that the balance of charge-transfer valence-bond states

and bandlike metallic states is sensitive to the surface polarization of the oxide. The fact that these results are greatly diminished at four or five layers indicates that this is a nanoscale effect. Preliminary investigations on Pd and Rh supported on the  $Al_T$  and  $O_T$  surfaces show similar modifications of the electronic structure, indicating that these changes may be general for transition metals on electronegative and electropositive surfaces.

While it is known that low-coordinated sites greatly enhance the reactivity of metal particles,<sup>10,11</sup> these results demonstrate the importance of metal-support charge transfer in predicting the properties at the metal surface, offering further support for the recent work of Chen and Goodman.<sup>15</sup> In addition, our findings suggest that increased reactivity at the perimeter of metal particles with diameters below 5 nm (Refs. 5, 6, 13, and 32) may be partially attributed to the strong metal-oxide coupling accessible at these boundaries. These concepts may be useful for applications as diverse as chemical sensors, fuel cells, and photochemical reactions.

We thank Sara E. Mason and Ilya Grinberg for discussions on CO adsorption energy corrections. This work was supported by the Air Force Office of Scientific Research, under Grant No. FA9550-04-1-0077, and the Office of Naval Research, under Grant No. N-000014-00-1-0372. Computational support was provided by the High-Performance Computing Modernization Office of the Department of Defense, the Defense University Research Instrumentation Program, and National Science Foundation under Grant No. 0131132. V.R.C. thanks IBM and ACS for support. A.M.K. was supported by Arkema Inc.

\*Electronic address: rappe@sas.upenn.edu

<sup>1</sup>C. Bozo *et al.*, *J. Catal.* **393**, 393 (2001).

<sup>2</sup>E. J. Walter *et al.*, *Surf. Sci.* **495**, 44 (2001).

<sup>3</sup>L. M. Molina and B. Hammer, *Phys. Rev. Lett.* **90**, 206102 (2003).

<sup>4</sup>R. Lindsay *et al.*, *Surf. Sci. Lett.* **547**, L859 (2003).

<sup>5</sup>M. Haruta, *Catal. Today* **36**, 153 (1997).

<sup>6</sup>E. S. Putna *et al.*, *Surf. Sci. Lett.* **391**, L1178 (1997).

<sup>7</sup>S. Roberts and R. J. Gorte, *J. Chem. Phys.* **93**, 5337 (1990).

<sup>8</sup>W. T. Petrie and J. M. Vohs, *J. Chem. Phys.* **101**, 8098 (1994).

<sup>9</sup>G. Mills *et al.*, *Chem. Phys. Lett.* **359**, 493 (2002).

<sup>10</sup>Z. L. Wang *et al.*, *Surf. Sci.* **380**, 302 (1997).

<sup>11</sup>J. W. Yoo *et al.*, *J. Catal.* **214**, 1 (2003).

<sup>12</sup>B. Yoon *et al.*, *J. Phys. Chem. A* **107**, 4066 (2003).

<sup>13</sup>M. Valden *et al.*, *Science* **281**, 1647 (1998).

<sup>14</sup>A. Sanchez *et al.*, *J. Phys. Chem. A* **103**, 9573 (1999).

<sup>15</sup>M. S. Chen and D. W. Goodman, *Science* **306**, 252 (2004).

<sup>16</sup>B. Hammer and J. K. Nørskov, *Surf. Sci.* **343**, 211 (1995).

<sup>17</sup>B. Hammer *et al.*, *Phys. Rev. Lett.* **76**, 2141 (1996).

<sup>18</sup>P. Hohenberg and W. Kohn, *Phys. Rev.* **136**, B864 (1964).

<sup>19</sup>W. Kohn and L. J. Sham, *Phys. Rev.* **140**, A1133 (1965).

<sup>20</sup>J. Toofan and P. R. Watson, *Surf. Sci.* **401**, 162 (1998).

<sup>21</sup>P. J. Eng *et al.*, *Science* **288**, 1029 (2000).

<sup>22</sup>L. Pauling and S. B. Hendricks, *J. Am. Chem. Soc.* **47**, 781 (1925).

<sup>23</sup>J. P. Perdew *et al.*, *Phys. Rev. B* **46**, 6671 (1992).

<sup>24</sup>B. Hammer *et al.*, *Phys. Rev. B* **59**, 7413 (1999).

<sup>25</sup>D. Vanderbilt, *Phys. Rev. B* **41**, R7892 (1990).

<sup>26</sup>H. J. Monkhorst and J. D. Pack, *Phys. Rev. B* **13**, 5188 (1976).

<sup>27</sup>W. E. Lee and K. P. D. Lagerlof, *J. Electron Microsc. Tech.* **2**, 247 (1985).

<sup>28</sup>P. J. Feibelman *et al.*, *J. Phys. Chem. B* **105**, 4018 (2001).

<sup>29</sup>I. Grinberg *et al.*, *J. Chem. Phys.* **117**, 2264 (2002).

<sup>30</sup>S. E. Mason *et al.*, *Phys. Rev. B* **69**, 161401(R) (2004).

<sup>31</sup>Y. Yourdshahyan *et al.*, *Proc. SPIE* **5223**, 223 (2003).

<sup>32</sup>U. Heiz *et al.*, *J. Am. Chem. Soc.* **121**, 3214 (1999).

<sup>33</sup>For our second order perturbation theory model the parameters were fit to our DFT calculations and are as follows:  $V_{\pi}^{top} = 10.93$ ,  $V_{\pi}^{hol} = 8.82$ ,  $V_{\sigma}^{top} = 7.53$ ,  $V_{\sigma}^{hol} = 2.59$ ,  $\alpha_{\pi}^{top} = 6.37$ ,  $\alpha_{\sigma}^{hol} = 8.97$ .